Chapter 1

TERRESTRIAL AND ASTROPHYSICAL SUPERFLUIDITY: COLD ATOMS AND NEUTRON MATTER

Alexandros Gezerlis
Department of Physics, University of Washington,
Seattle, Washington 98195 USA

J. Carlson
Theoretical Division, Los Alamos National Laboratory,
Los Alamos, New Mexico 87545 USA

Abstract: After a brief historical overview of superfluidity in connection with neutron matter and cold fermionic atoms, we discuss the commonalities between these two systems as well as their relevance to the physics of neutron star crusts. We then present the methodological tools we use to attack the many-body problem, comparing Quantum Monte Carlo to mean-field theory and to the analytic expectations at weak coupling. We review recent results on the equation of state and the pairing gap of cold atoms and neutron matter and contrast them with a variety of calculations by other groups. We conclude by giving a few directions of possible future inquiry.

1.   Historical Overview

One could fill volumes (and many people have done so) writing on the history of superfluidity and superconductivity. Our goals are much humbler: we only wish to connect the pairing found in neutron matter with recent cold fermionic atom experiments. Thus, our ever-shifting kaleidoscope (which relies mainly on Refs. [1, 2, 3, 4]) by construction passes over in silence discoveries that are major, but do not bear a direct relation to the physics of neutron-star crusts. The natural way to start such a brief historical overview is by mentioning Heike Kamerlingh Onnes, who in 1908 liquefied ^{4}He, at 4.2 K. Onnes mentions in

his 1913 Nobel lecture [5] that the behavior of ^{4}He at an even colder temperature, 2.2 K, presents an interesting problem, which "could possibly be connected with the quantum theory" (note that this was said in 1913). Onnes had already realized that there was something peculiar about that temperature. Instead of staying on the subject of bosonic systems, he used ^{4}He to cool down mercury, discovering superconductivity (a drop of the resistivity to non-measurable values) at 4.1 K in that system.

Then, in 1925, when the statistics different particles follow was still unresolved, Einstein predicted the phenomenon now known as Bose-Einstein condensation (BEC), according to which below a certain temperature a finite fraction of the total number of particles occupies the lowest-energy single-particle state. In 1927, Keesom and Wolfke made the distinction between the two phases of ^{4}He above and below the λ transition point around 2.2 K. In 1938 Kapitsa and, separately, Allen & Misener discovered superfluidity (a drop of the viscosity to essentially zero) using ^{4}He. A year later, Kapitsa managed to get Lev Davidovich Landau released from prison, with the hope that he would be able to provide a theoretical explanation of this new effect.

In an apparently unrelated context, Baade and Zwicky (in 1934, only two years after the discovery of the neutron) proposed the idea of high-density and small-radius *neutron stars* which would be much more gravitationally bound than ordinary stars and would be formed in supernova explosions. On the terrestrial front, Fritz London was the first person to suggest that superconductivity and superfluid flow in liquid helium were macroscopic quantum phenomena. Then in 1950 Ginzburg and Landau proposed what seemed to be a phenomenological theory by introducing a complex pseudo wave function ψ as an order parameter in Landau's general theory of second-order phase transitions. In 1957 the epoch-making microscopic Bardeen-Cooper-Schrieffer (BCS) theory of superconductors was put forward, allowing one to calculate the pairing gap Δ. In it, the electron-phonon interaction causes an instability in the Fermi-sea with respect to the formation of what are now called *Cooper pairs*. Just two years later, Gorkov showed that the Ginzburg-Landau theory was a limiting form of the BCS theory around the critical temperature, in which ψ is directly proportional to the gap Δ.

In the meantime, Bohr, Mottelson, and Pines had already (in 1958) made an analogy between the low-energy spectra of nuclei and of the electrons in a superconducting metal. In 1959 Migdal, [6] in what was essentially a throw-away comment, noted that the "superfluidity of nuclear matter may lead to some interesting cosmological phenomena if stars exist which have neutron cores. A star of this type would be in a superfluid state with a transition temperature corresponding to 1 MeV". Thus, the study of superfluidity in infinitely extended nuclear systems (such as neutron-star matter or nuclear matter) predates the 1967 discovery of pulsars, which were identified as rapidly rotating magnetic neutron stars the next year. A few years after its formation, the relevant part of a neutron star is expected to have a temperature from 10^6 K to 10^9 K, i.e. a small fraction of the pairing gap.

Enter unconventional superfluidity: in 1972 Lee, Osheroff, and Richardson observed superfluid phases of ^{3}He (a fermionic atom) at a transition temperature of around 2.7 mK, three orders of magnitude lower than for ^{4}He. Just weeks after the discovery of the superfluid, Anthony Leggett extended previous work of his and identified the states seen in the new data. In a similarly untypical development, in 1986 Bednorz and Müller discovered superconductivity at 35 K in a barium lanthanum copper oxide, initiating the era of what

are now known as high-T_c superconductors. Currently, the highest-T_c superconductor is mercury thallium barium calcium copper oxide at 138 K. In contradistinction to the case of ^{3}He, a comprehensive theory of high-T_c superconductors is still being sought.

In parallel developments, in 1980 Leggett showed that for fermions the limits of tightly bound molecules and long-range Cooper pairs are connected in a smooth crossover (BCS-BEC crossover). On the bosonic side, 1995 saw the first realization of Bose-Einstein condensation in dilute vapors of alkali atoms. Most of the physics involved was governed by mean-field interactions, and could be well described by the Gross-Pitaevskii equation. As an experimental discovery it was very important in and for itself, providing a clear realization of the phenomenon that Einstein had theoretically predicted 70 years earlier. But the methods involved in this research program on alkali atoms (magnetic trapping, evaporative cooling, sympathetic cooling, optical trapping, and Feshbach resonances) were then used to examine fermionic gases (in some cases, by the same research groups), the first example of quantum degeneracy in trapped Fermi gases being ^{40}K in 1999 at JILA. In November 2003, three groups reported the realization of Bose-Einstein condensates of molecules composed of fermionic atoms, and soon after that the observations were extended throughout the entire BEC-BCS crossover. One of the high points (possibly *the* high point) in the ensuing explosion of research was the demonstration of fermionic superfluidity and phase coherence at MIT in April 2005. These phenomena, just like superfuidity in neutron matter, are characterized by strong interactions and cannot be dealt with satisfactorily in a mean-field theory framework. However, in contradistinction with neutron matter, cold atoms can be directly probed in the laboratory and can therefore help constrain nuclear theory.

2. Mise-en-scène

The materials already referred to as high-T_c superconductors are so called because they have the highest T_c's (in an absolute scale) currently known on earth. However, if we take a different view and speak instead in terms of relative temperatures, comparing the critical temperature with a temperature that sets the scale in each system (the Fermi temperature T_F), things look different. In Table 1 we have summarized some results for fermionic systems. Neutron matter and ultracold atomic gases are separated by 17 orders of magnitude: however, in terms of their corresponding Fermi temperatures, their critical temperatures are

Table 1. Typical values for the transition temperature T_c, and the ratio of the transition temperature to the Fermi temperature T_c/T_F, for various fermionic superfluids or superconductors.

	T_c	T_c/T_F
Conventional superconductors	5 K	$5 \cdot 10^{-5}$
^{3}He	2.7 mK	$5 \cdot 10^{-4}$
High-T_c superconductors	100 K	10^{-2}
Neutron matter	10^{10} K	0.1
Atomic Fermi gases	200 nK	0.2

very large, essentially of comparable magnitude. This is the reason both these systems can be viewed as "high-temperature superfluids", even though one occurs at very small and the other at very large temperature. Since the pairing gap Δ is roughly proportional to the critical temperature T_c, both these systems also exhibit very strong pairing, the strongest ever observed before in nature or experimented with in the laboratory. As we shall see below, in cold fermionic atoms the particle-particle interactions can be tuned experimentally, allowing one to examine a whole range of new phenomena, thus also mimicking the setting of low-density neutron matter, which is beyond direct experimental reach. In order to make this more tangible, let us begin with Schwinger and Bethe's "shape-indendent formula", used to describe s-wave scattering:

$$k \cot \delta = -\frac{1}{a} + \frac{1}{2}k^2 r_e \, , \tag{1}$$

In this expression, k is the momentum and δ is the s-wave phase shift. Knowing the latter gives us the scattering cross section, which is experimentally observable. This formula implies that low-energy scattering provides information about only these two parameters: the scattering length a and the effective range r_e. Thus, the cross section is independent of the details of the potential. Let us now discuss some specifics of our two systems and their interparticle interactions.

2.1. Ultracold Atomic Gases

For ultracold fermionic atoms at low temperature, [3, 4, 7, 8] the superfluid phase arises only in the presence of interactions. The first batch of fermionic experiments was done with an equal mixture of the two lowest hyperfine states, conventionally referred to as hyperfine states $|1\rangle$ and $|2\rangle$, of ^{6}Li or ^{40}K confined optically in a dipole trap.

The atom-atom interaction is quite complicated, though sophisticated models such as the Aziz potential for helium are often replaced by the simplified Lennard-Jones form. For cold alkali gases we have a van der Waals length $r_c \approx 50 - 100$ Å, but in the quantum degenerate regime the interparticle spacing is at least a few thousand Å, i.e. the interparticle spacing is significantly larger than the characteristic length of the interaction. In a broad Feshbach resonance we have $k_F r_e \ll 1$, where k_F is the Fermi wave vector (connected to the number density via $\rho = k_F^3/(3\pi^2)$), so at fixed density the effective-range can be taken to be very small, essentially zero (though it may be possible to use narrow and wide resonances in cold atoms to study the case of varying r_e experimentally, [9] and thus directly simulate neutron matter).

What was critically new in the fermionic cold atom experiments of the last decade was the ability to vary the interaction strength (the scattering length a) across a resonance, through a regime known as "unitarity". This system is very interesting, since it is both dilute (i.e. the range of the interatomic potential is much smaller than the interparticle distance) and strongly interacting (i.e. the scattering length is much larger than the interparticle distance). In this regime, all the length scales associated with interactions drop out of the problem and the system is expected to exhibit universal behavior, [10] i.e. a non-dependence on the specifics of the interatomic potential, which is why, in principle, any fermionic atom can be used to perform such experiments. The unitary Fermi gas has been

the subject of intensive theoretical study, both in the homogeneous case, and for the case of a trapped gas.

Let us now move on to observable many-body properties that can be and have been measured in such experiments. Experiments using ^{6}Li at Duke University [8] and at ENS [11] have measured the ground-state energy of the system, essentially finding it to be in agreement with Quantum Monte Carlo predictions [12, 13, 14, 15, 16] (very recent experimental results from MIT [17] and fermion-sign-free theoretical values [18] change this picture only quantitatively). The ground-state energy per particle is conventionally given in units of the energy of a free Fermi gas at the same density $E_{FG} \equiv 3E_F/5 = 3\hbar^2 k_F^2/(10m)$ as $E = \xi E_{FG}$. Other experiments at MIT and Rice probed lithium gases with population imbalance (also called "polarized" gases). An MIT experiment [19] established the phase diagram of a polarized gas, revealing spatial discontinuities in the spin polarization. This experiment was then used [20] to extract the pairing gap, which was found to be approximately half of the Fermi energy E_F, in good agreement with QMC calculations [14]. (Similarly to the case of the ground-state energy, the gap is conventionally given in units of E_F as $\Delta = \eta E_F$). The MIT group went on to use RF spectroscopy to independently determine the gap, finding it to be in agreement with the afore-mentioned calculation and extraction. [21]

2.2. Neutron-Star Matter

The neutrons in the inner crust are expected to pair in the $^1S_0$ channel, [22, 23] but superfluidity in this channel will probably exhibit gap closure before reaching the core. Let us note that even though, as we already pointed out, the temperature of the crust is from 10^6 K to 10^9 K the neutron gas is still superfluid because the critical temperature is expected to be larger, approximately 10^{10} K (see Table 1). The first-order approximation to this superfluid gas embedded in a lattice of nuclei is to consider infinite pure neutron matter and examine the effect of the ion lattice only at a later stage. For many decades, there has been a large spread of predictions of the $^1S_0$ pairing gap even for this idealized pure system, which we discuss in a later section. This spread is mainly due to the differences in the many-body schemes employed: dilute neutron matter is a system that is very strongly paired, meaning that all perturbative approaches fail, and most diagrammatic techniques in general have no way of specifying why any specific class of diagrams should be dominant.

Even so, dilute neutron matter is simple when compared to the general nuclear many-body problem. To see this, we turn turn our attention to the neutron-neutron interaction. In general it is complicated, necessitating sophisticated models (such as the Argonne $v18$ potential) to describe it. It has a strong dependence on quantum numbers such as total spin S and isospin T. In local potentials it has a strongly repulsive core at distances of ~ 0.5 fm, as well as an electromagnetic (in the case of neutrons, magnetic-moment) term, and one-pion exchange at large distances and intermediate-range spin-dependent attraction which is dominated by two-pion exchange. However, as in the case of cold fermionic atoms, there are some simplifications: in very dilute neutron matter the density (or k_F) goes to zero, making all the terms in the interaction apart from the s-wave channel drop off. In contradistinction to the case of cold atoms, the neutron-neutron effective range is not necessarily small in comparison to the interneutron spacing: $r_e = 2.7$ fm (with $k_F r_e$ going from 0 to 1.5).

Another critical distinction is that for neutrons in a neutron-star crust the scattering length is not at our disposal, being fixed, instead, at the value of $a = -18.5$ fm, larger than the interparticle spacing ($k_F a$ goes from 0 to -10).

Let us now move on to possible observational evidence of neutron-star matter pairing. Superfluidity in a neutron star is often used to explain its dynamical and thermal evolution. Starting with the former: the main example of this is given by pulsar post-glitch timing observations. For some pulsars, even though their angular frequency decreases slowly but steadily, there also occur sudden and rapid speed-ups of the frequency (called glitches), which are in their turn followed by a gradual decay of the increased frequency. The dominant phenomenological model holds that the speed-up is triggered by a "starquake" in the crust. The crust speed-up is rapidly communicated to the charged particles by the strong magnetic field. However, the response of the neutron superfluid to the speed-up is considerably slower and proceeds via electron scattering by the normal fluid cores of the vortex lines in the rotating superfluid. (This model was, astonishingly, proposed immediately after the first Vela pulsar glitch.) [24]

The other commonly referred to aspect in which pairing is important has to do with neutron-star cooling: observations of cooling quiescent neutron stars provide evidence for the existence of a neutron superfluid throughout the inner crust. [25] This is so because the specific heat of a superfluid is exponentially suppresed. Furthermore, in the presence of a neutron $^1S_0$ gap, the neutron-neutron bremsstrahlung reaction rate is also suppressed. Finally, Cooper-pair breaking/formation neutrino emission processes that occur near the transition temperature are also relevant to the cooling of neutron stars, though due to the small size of the crust this happens only during the first few hundred years of evolution, i.e. during the crust's thermal relaxation. Cooper-pair breaking/formation calculations have recently introduced vector current conservation, leading to the conclusion that the vector part of the contribution to this process is strongly suppressed, though the axial part is only slightly modified. These three factors (specific heat, bremsstrahlung, pair breaking/formation) have been incorporated in a recent minimal-cooling paradigm calculation, [26] which showed that different $^1S_0$ pairing gap calculations lead to only slight quantitative differences in the cooling curves of young neutron stars. All these factors show the importance of superfluidity in neutron matter, but do not probe the magnitude of the pairing gap. The situation in that regard may be different as regards a new mechanism that makes use of superfluid phonons. [27] Whether this mechanism is competitive to the heat conduction by electrons in magnetized neutron stars or not is a question that is directly correlated to the size of the gap.

Finally, let us point out that, outside the observational realm, neutron matter computations also hold significance in the context of traditional nuclear physics: equation of state results at densities close to the nuclear saturation density have been used for some time to constrain Skyrme and other density functional approaches to heavy nuclei, [28] while the density-dependence of the $^1S_0$ gap in low-density neutron matter has recently also been used to constrain Skyrme-Hartree-Fock-Bogoliubov treatments in their description of neutron-rich nuclei [29].

3. Quantum Many-Body Methods

In the series of works reviewed in the present text, both cold atoms and neutron matter were attacked using the same methodology: Quantum Monte Carlo many-body simulations. Such methods have been used for decades to calculate the energies of many systems, e.g. liquid helium. In such systems, however, QMC methods were unable to provide the pairing gaps, because of the vast difference in scale between the energy of the entire system (of the order of eV's per particle) and the pairing gap (of the order of meV). Thus, in a fortuitous turn of events, the same feature of strongly paired fermionic systems (the large pairing gap) that precludes the application of mean-field theories, is precisely the reason that allows many-body simulation techniques to be used. Before giving a few technical details on how Green's Function Monte Carlo works, we first go over the analytically exact expectations for quantum many-body theory, that we know any correct new approach should recover as a limiting case. After that we discuss BCS mean-field theory, which is not expected to be exact in the strongly paired regime, but even so is a useful benchmark with which to compare other theories.

3.1. Weak coupling

At extremely low densities ($|k_F a| << 1$) the effective coupling between two fermions is weak and matter properties can be calculated analytically. The ground-state energy of normal (i.e. non-superfluid) matter in this regime was calculated by Lee and Yang in 1957: [30]

$$\frac{E}{E_{FG}} = 1 + \frac{10}{9\pi} k_F a + \frac{4}{21\pi^2} \left(11 - 2\ln 2\right) (k_F a)^2 \ , \tag{2}$$

where E_{FG} is the energy of a free Fermi gas at the same density as the interacting gas. While this expression ignores the contributions of superfluidity, these are exponentially small in $(1/k_F a)$. In the next section we compare these results to QMC calculations for $|k_F a| \geq 1$.

The pairing gap at weak coupling is also known analytically. The mean-field BCS approach described below [Eq. 9] reduces in this limit to:

$$\Delta^0_{BCS}(k_F) = \frac{8}{e^2} \frac{\hbar^2 k_F^2}{2m} \exp\left(\frac{\pi}{2ak_F}\right) \ . \tag{3}$$

However, as was shown in 1961 by Gorkov and Melik-Barkhudarov, [31] the BCS result acquires a finite polarization correction even at weak coupling, yielding a reduced pairing gap:

$$\Delta^0(k_F) = \frac{1}{(4e)^{1/3}} \frac{8}{e^2} \frac{\hbar^2 k_F^2}{2m} \exp\left(\frac{\pi}{2ak_F}\right) \ . \tag{4}$$

Thus, the polarization corrections reduce the mean-field BCS result by a factor of $1/(4e)^{1/3} \approx 0.45$. Interestingly, if one treats the polarization effects at the level of sophistication used in the work of Gorkov and Melik-Barkhudarov, this factor changes with $k_F a$ [32], though there is no *a priori* reason to expect such an approach to be valid at stronger coupling ($k_F a$ of order 1 or more). Calculating the pairing gap in this region has been an onerous task, as can be seen from the multitude of publications devoted to this subject in the past few decades.[22, 23, 33, 34, 35, 36, 37, 38, 39, 40, 41, 42, 43]

3.2. BCS in the continuum and in a box

As the coupling strength increases, we expect the BCS mean-field theory to become more accurate. In the BCS-BEC transition studied in cold atoms, the BCS theory goes correctly to the two-body bound state equation in the deep BEC regime. Though we do not expect BCS results to be quantitatively reliable in the regime of interest for neutron-star crusts, BCS theory provides a standard basis of comparison for our *ab initio* results and also allows us to analyze finite-size effects in the QMC simulations in a simple way. Within the BCS formalism the wave function is:

$$|\psi\rangle = \prod_{\mathbf{k}}(u_{\mathbf{k}} + v_{\mathbf{k}}c_{\mathbf{k}\uparrow}^{\dagger}c_{-\mathbf{k}\downarrow}^{\dagger})|0\rangle \; , \tag{5}$$

where $u_{\mathbf{k}}^2 + v_{\mathbf{k}}^2 = 1$. A variational minimization of the expectation value of the Hamiltonian for an average partice number (or density) leads to the gap equation:

$$\Delta(\mathbf{k}) = -\sum_{\mathbf{k}'}\langle\mathbf{k}|v|\mathbf{k}'\rangle\frac{\Delta(\mathbf{k}')}{2E(\mathbf{k}')} \; , \tag{6}$$

where the elementary quasi-particle excitations of the system have energy:

$$E(\mathbf{k}) = \sqrt{\xi(\mathbf{k})^2 + \Delta(\mathbf{k})^2} \tag{7}$$

and $\xi(\mathbf{k}) = \epsilon(\mathbf{k}) - \mu$, where the chemical potential is μ and $\epsilon(\mathbf{k}) = \frac{\hbar^2 k^2}{2m}$ is the single-particle energy of a particle with momentum $\mathbf{k}$. The chemical potential is found by solving the gap equation together with the equation that provides the average particle number:

$$\langle N\rangle = \sum_{\mathbf{k}}\left[1 - \frac{\xi(\mathbf{k})}{E(\mathbf{k})}\right] \; . \tag{8}$$

When interested in the $^1S_0$ gap for neutron matter, it is customary to perform partial-wave expansions of the potential and the gap functions, as well as an angle-average approximation. Thus, Eq. (6) takes the form:

$$\Delta(k) = -\frac{1}{\pi}\int_0^\infty dk' \, k'^2 \frac{v(k,k')}{E(k')}\Delta(k') \; , \tag{9}$$

where the potential matrix element is:

$$v(k,k') = \int_0^\infty dr \, r^2 j_0(k'r)V(r)j_0(kr) \; . \tag{10}$$

Similarly, Eq. (8) becomes:

$$\rho = \frac{1}{2\pi^2}\int_0^\infty dk \, k^2 \left(1 - \frac{\xi(k)}{E(k)}\right) \; . \tag{11}$$
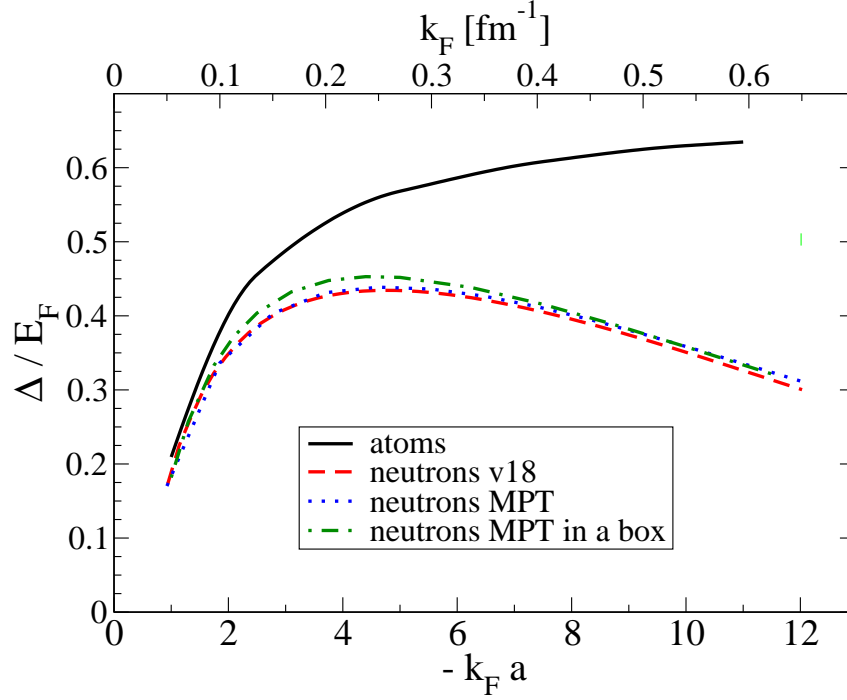
Figure 1. BCS pairing gap Δ divided with the Fermi energy E_F, versus the Fermi momentum k_F for cold atoms (solid line), neutrons with AV18 (dashed line), neutrons with a modified Pöschl-Teller potential (dotted line) tuned to have the same scattering length and effective range as AV18. At low density all curves are identical for practical purposes. Also shown is the solution of the BCS problem in a periodic box using the modified Pöschl-Teller potential for 66 neutrons (dash-dotted line).

These equations are one dimensional, and thus simple to treat numerically. The density equation can be decoupled from the gap equation only when $\Delta/\mu << 1$; this is not the case for the density regime we are considering.

In Ref. [15] Eq. (9) was solved in tandem with Eq. (11) for a modified Pöschl-Teller (MPT) potential:

$$v(r) = -v_0 \frac{2\hbar^2}{m} \frac{\nu^2}{\cosh^2(\nu r)} \ , \qquad (12)$$

where v_0 and ν are parameters which can be tuned so that this potential reproduces any desirable scattering length and effective range. The potential in Eq. (12) clearly has no repulsive core, making it amenable to a straightforward iterative solution. In this reference the potential was tuned so that the effective range is considerably shorter than the average interparticle spacing and at the same time the product $k_F a$ was varied from -1 to -10. The result is the solid line marked as "atoms" in Fig. 1. If $k_F a$ is taken to be infinite (the unitarity regime, unattainable in neutron star crusts) the BCS limiting value turns out to be 0.69.

In Ref. [44] Eq. (9) was then solved together with Eq. (11) using the same MPT

potential but the potential parameters were tuned so as to reproduce the neutron-neutron scattering length $a \approx -18.5$ fm and effective range $r_e \approx 2.7$ fm, the result also being shown in Fig. 1 (dotted line). The same exercise was repeated for a more realistic microscopic potential, namely the $^1S_0$ channel of the Argonne v18 [45] potential that contains a strong short-range repulsion. This calculation is greatly simplified if one uses the method described in Ref. [46], thereby transforming the problem into a quasilinear one; the result is the dashed line. For all the densities considered, the results of solving Eqs. (9) and (11) with the appropriately tuned MPT potential and with the Argonne v18 potential are virtually indistinguishable.

The modified Pöschl-Teller potential can also be used in a calculation for finite average particle number. This is interesting because the Quantum Monte Carlo simulations discussed below are performed in a periodic simulation volume. This means that, in principle, there may exist considerable finite-size effects: since the simulation cannot be performed in the thermodynamic limit, the question arises of how close to it one is. Refs. [15, 44, 47] solved Eqs. (6) and (8) for $\langle N \rangle$ from 20 to 200, in periodic boundary conditions in a cubic box of volume L^3:

$$\mathbf{k_n} = \frac{2\pi}{L}(n_x, n_y, n_z) \ . \tag{13}$$

There it was found that $\langle N \rangle = 66$ is very close to the thermodynamic limit. In Fig. 1 we show the results of solving the BCS gap equation Eq. (6) in a periodic box along with the particle-number conserving Eq. (8) for $\langle N \rangle = 66$ (dash-dotted line); as already noted, the discrepancy between that curve and the continuum result is small. Given this finite-size analysis, the Quantum Monte Carlo results shown in the rest of this review were performed using approximately 66 particles in periodic boundary conditions.

3.3. Quantum Monte Carlo

The Hamiltonian for cold atoms and neutron matter at low densities is:

$$\mathcal{H} = \sum_{k=1}^{N}\left(-\frac{\hbar^2}{2m}\nabla_k^2\right) + \sum_{i<j'} v(r_{ij'}) \ . \tag{14}$$

where N is the total number of particles. In the case of cold atoms the interaction only acts between opposite spin pairs and is of the form shown in Eq. (12). The neutron-neutron interaction is more complicated but still simple if one considers the AV4 formulation: [48]

$$v_4(r) = v_c(r) + v_\sigma(r)\boldsymbol{\sigma}_1 \cdot \boldsymbol{\sigma}_2, \tag{15}$$

In the case of $S=0$ (singlet) pairs this gives:

$$v_S(r) = v_c(r) - 3v_\sigma(r) \ . \tag{16}$$

However, it also implies an interaction for $S=1$ (triplet) pairs:

$$v_P(r) = v_c(r) + v_\sigma(r) \ . \tag{17}$$

Ref. [44] explicitly included such p-wave interactions in the same-spin pairs (the contribution of which was small even at the highest density considered), and perturbatively corrected the $S = 1, M_S = 0$ pairs to the correct p-wave interaction.

In these calculations it is customary to first employ a standard Variational Monte Carlo simulation. This approach uses Monte Carlo integration to minimize the expectation value of the Hamiltonian:

$$\langle H \rangle_{VMC} = \frac{\int d\mathbf{R}\Psi_V(\mathbf{R})H\Psi_V(\mathbf{R})}{\int d\mathbf{R}|\Psi_V(\mathbf{R})|^2} \geq E_0 \ . \tag{18}$$

thereby optimizing a variational wave function Ψ_V.

At a second stage, the output of the Variational Monte Carlo calculation is used as input in a fixed-node Green's Function Monte Carlo simulation, which projects out the lowest-energy eigenstate Ψ_0 from a trial (variational) wave function Ψ_V. This it does by treating the Schrödinger equation as a diffusion equation in imaginary time τ and evolving the variational wave function up to large τ. The ground state is evaluated from:

$$\begin{aligned} \Psi_0 &= \exp[-(H - E_T)\tau]\Psi_V \\ &= \prod \exp[-(H - E_T)\Delta\tau]\Psi_V, \end{aligned} \tag{19}$$

evaluated as a branching random walk. The short-time propagator is usually taken as

$$\exp[-H\Delta\tau] = \exp[-V\Delta\tau/2]\exp[-T\Delta\tau]\exp[-V\delta\tau/2], \tag{20}$$

which is accurate to order $(\Delta\tau)^2$.

The fixed-node calculation gives a wave function Ψ_0 that is the lowest-energy state with the sames nodes (surface where $\Psi = 0$) as the trial state Ψ_V. The resulting energy E_0 is an upper bound to the true ground-state energy. The variational wave function Ψ_V has a Jastrow-BCS form (see below), and contains a variety of parameters, many of which affect the nodal surfaces. Since the fixed-node energy is an upper bound to the true ground state, these parameters can be optimized to give the best approximation to the ground-state wave function. In order to optimize these variational parameters, they were included as slowly diffusing coordinates in a preliminary GFMC calculation. The parameters evolve slowly in imaginary time, equilibrating around the lowest-energy state consistent with the chosen form of the trial wave function.[12]

The ground-state energy E_0 can be obtained from:

$$E_0 = \frac{\langle \Psi_V|H|\Psi_0 \rangle}{\langle \Psi_V|\Psi_0 \rangle} = \frac{\langle \Psi_0|H|\Psi_0 \rangle}{\langle \Psi_0|\Psi_0 \rangle}. \tag{21}$$

In all these Quantum Monte Carlo superfluid simulations the trial wave function was taken to be of the Jastrow-BCS form with fixed particle number:

$$\Psi_V = \prod_{i\neq j} f_P(r_{ij}) \prod_{i'\neq j'} f_P(r_{i'j'}) \prod_{i,j'} f(r_{ij'}) \mathcal{A}[\prod_{i<j'} \phi(r_{ij'})] \tag{22}$$

and periodic boundary conditions. The primed (unprimed) indices correspond to spin-up (spin-down) neutrons. The pairing function $\phi(r)$ is a sum over the momenta compatible with the periodic boundary conditions. In the BCS theory the pairing function is:

$$\phi(r) = \sum_{\mathbf{n}} \frac{v_{\mathbf{k_n}}}{u_{\mathbf{k_n}}} e^{i\mathbf{k_n}\cdot\mathbf{r}} = \sum_{\mathbf{n}} \alpha_n e^{i\mathbf{k_n}\cdot\mathbf{r}} \ , \tag{23}$$

and can be parametrized with a short- and long-range part as in Ref. [12]:

$$\phi(\mathbf{r}) = \tilde{\beta}(r) + \sum_{\mathbf{n},\, I \leq I_C} \alpha_I e^{i\mathbf{k_n}\cdot\mathbf{r}} \,, \tag{24}$$

where $I = n_x^2 + n_y^2 + n_z^2$ using the parameters defined in Eq. (13). The Jastrow part is usually taken from a lowest-order-constrained-variational method [49] calculation described by a Schrödinger-like equation:

$$-\frac{\hbar^2}{m}\nabla^2 f(r) + v(r)f(r) = \lambda f(r) \tag{25}$$

for the opposite-spin $f(r)$ and by the corresponding equation for the same-spin $f_P(r)$. Since the $f(r)$ and $f_P(r)$ are nodeless, they do not affect the final result apart from reducing the statistical error. The fixed-node approximation guarantees that the result for one set of pairing function parameters in Eq. (24) will be an upper bound to the true ground-state energy of the system. As mentioned above, the parameters are optimized in the full QMC calculation, providing the best possible nodal surface, in the sense of lowest fixed-node energy, with the given form of trial function. This upper-bound property is made use of in an attempt to get as close to the true ground-state energy as possible.

4.   Equation of state

The $T = 0$ equations of state for cold atoms and neutron matter of Ref. [15] are compared in Fig. 2. The horizontal axis is $k_F a$, with the equivalent Fermi momentum k_F for neutron matter shown along the top. The vertical axis is the ratio of the ground-state energy to the free Fermi gas energy (E_{FG}) at the same density; it must go to one at very low densities and decrease as the density increases and the interactions become important. The curve at lower densities shows the analytical result by Lee and Yang we mentioned in an earlier section. The QMC results shown in this figure seem to agree with the trend implied by the Lee-Yang result (which has not been extended to even higher density because of its weak-coupling nature). The neutron matter and cold atom equations of state are very similar even for densities where the effective range is comparable to the interparticle spacing. Hence, our earlier hope that cold-atom experiments can tell us something rather directly about the neutron-matter equation of state is now more than just a hope. Near $k_F a = -10$ the energy per particle is not too far from QMC calculations and measurements of the ratio ξ of the unitary gas energy to E_{FG} shown as an arrow on the right (it corresponds to $k_F a = \infty$); previous calculations give $\xi \approx 0.4$ (however, as mentioned above, see also Refs. [17, 18]). At larger densities the cold-atom and neutron matter results start to diverge from each other. This is due to two separate factors: i) the neutron finite effective range, and ii) the fact that the neutron results also incorporate an early attempt to correct the $S = 1$, $M_S = 0$ pairs. When the density is very low, the s-wave contribution is dominant so cold atoms and neutron matter agree very well. At higher densities the energy is higher with the contribution of the p-wave interaction.

We also compare our neutron matter QMC AV4 results from Ref. [44] for the ground-state energy to other calculations extending to larger Fermi momenta. Let us note that
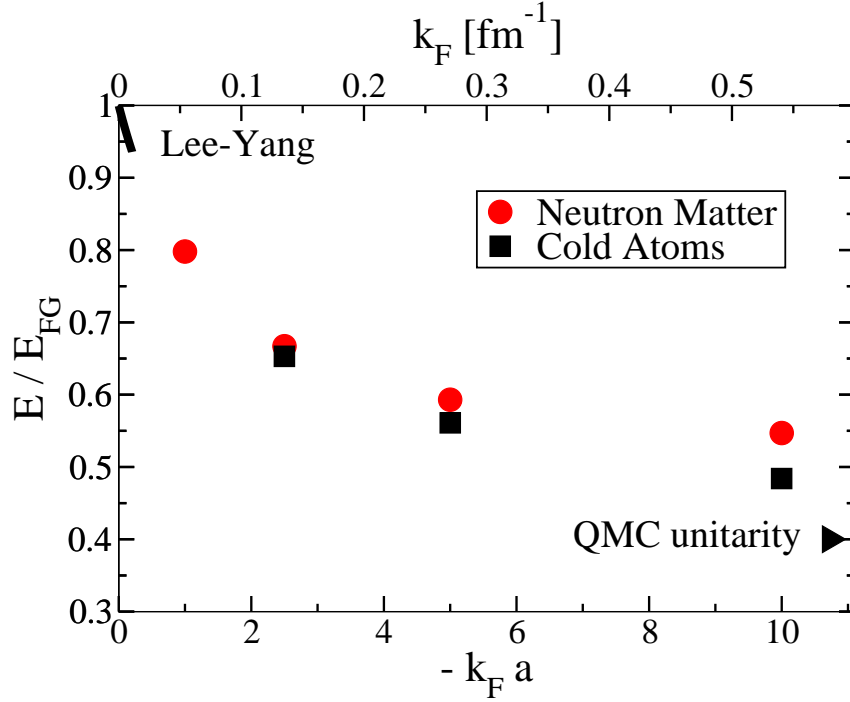
Figure 2. Quantum Monte Carlo equation of state for cold atoms (squares) and neutron matter (circles). Also shown are the analytic expansion of the ground-state energy of a normal fluid (line) and the Quantum Monte Carlo result at unitarity (arrow).

these are slightly different (larger) than the values shown in Fig. 2 because of i) including same-spin p-wave contributions, and ii) a more refined approach to dealing with the $S = 1$, $M_S = 0$ pairs. For the highest density examined, $k_F a = -10$, this change is approximately 7%, while for $k_F a = -5$ it is only 1%. Nonperturbative corrections at the highest density considered could reduce the difference between the s-wave interaction and AV4 results slightly. In Fig. 3 the results of Ref. [44] are compared to (approximate) variational hypernetted-chain calculations by Friedman and Pandharipande [50], and another calculation by Akmal, Pandharipande, and Ravenhall (APR) [51]. Also included are two Green's Function Monte Carlo results for 14 neutrons with more complete Hamiltonians [52], a result following from a Brueckner-Bethe-Goldstone expansion [55], a difermion EFT result (shown are the error bands) [53], the latest Auxiliary-Field Diffusion Monte Carlo (AFDMC) result (discussed below) [41], a Dirac-Brueckner-Hartree-Fock calculation [54], a lattice chiral EFT method at next to leading order [56] (see also Ref. [57]), and an approach that makes use of chiral N^2LO three-nucleon forces.[59] Of these, Refs. [51], [41], and [59] include a three-nucleon interaction, though at the densities considered, these are not expected to be significant. Qualitatively all of these results agree within 20%.
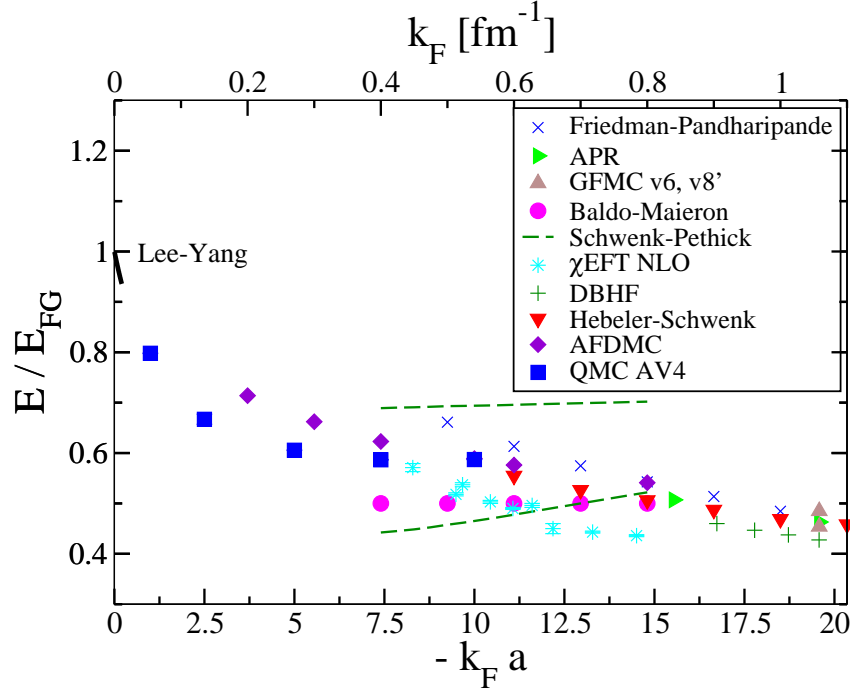
Figure 3. Equation of state for neutron matter compared to various previous results. Despite quantitative discrepancies, all calculations give essentially similar results. Our lowest density corresponds to $k_F a = -1$.

5. Pairing gap

In Fig. 4 we plot the pairing gap as a function of $k_F a$ for both cold atoms and neutron matter, taken from Ref. [15]. The Quantum Monte Carlo pairing gaps are arrived at from the ground-state energy, through the use of the odd-even staggering formula:

$$\Delta = E(N+1) - \frac{1}{2}\left[E(N) + E(N+2)\right] , \qquad (26)$$

where N is an even number of particles. BCS calculations are shown as solid lines, and QMC results are shown as points with error bars. QMC pairing gaps are shown from calculations of $N = 66 - 68$ particles. For very weak coupling, $-k_F a << 1$, the pairing gap is expected to be reduced from the BCS value by the polarization corrections calculated by Gorkov and Melik-Barkhudarov, $\Delta/\Delta_{BCS} = (1/4e)^{1/3}$, as mentioned in an earlier section (Eq. (4)). Because of finite-size effects, it is difficult to calculate pairing gaps using QMC in the weak coupling regime. The QMC calculations at the lowest density, $k_F a = -1$, are roughly consistent with this reduction from the BCS value. At slightly larger yet still small densities, where $-k_F a = \mathcal{O}(1)$ but $k_F r_e << 1$ for neutron matter, one would expect the pairing gap to be similar for cold atoms and neutron matter. The results at $k_F a = -2.5$, where $k_F r_e \approx 0.35$, support this expectation. Beyond that density the effective range becomes important and the QMC results are significantly reduced in relation to the cold atoms
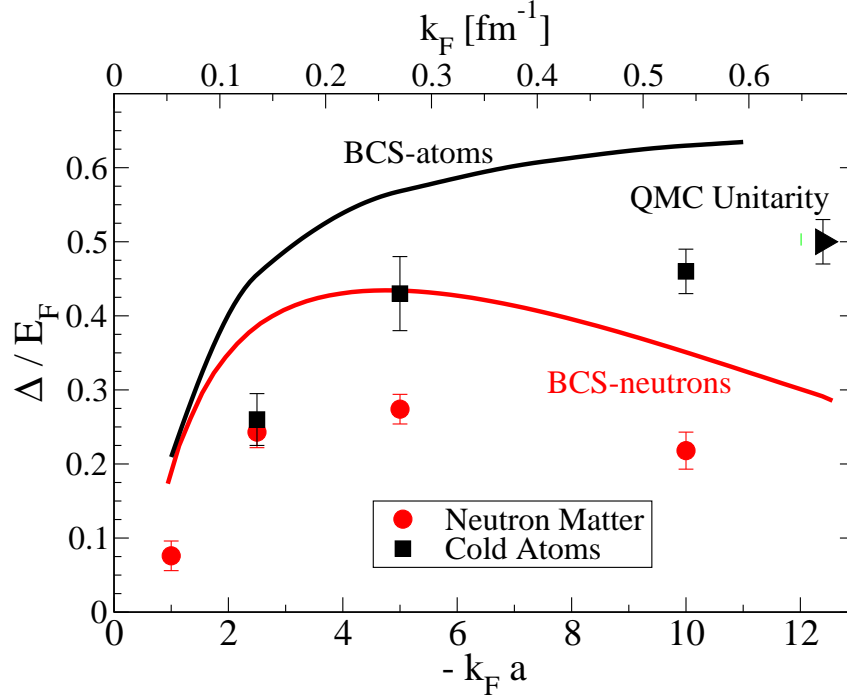
Figure 4. Superfluid pairing gaps versus $k_F a$ for cold atoms ($r_e \approx 0$) and neutron matter ($|r_e/a| \approx 0.15$). BCS (solid lines) and QMC results (points) are shown.

where $r_e \approx 0$.

In cold atoms, the suppression from BCS is reduced as the density increases, with a smoothly growing fraction of the BCS results as we move from the BCS to the BEC regime. At unitarity the measured pairing gaps [19, 20, 21] are 0.45(0.05) of the Fermi energy, for a ratio $\Delta/\Delta_{BCS} \approx 0.65$, in agreement with predictions by QMC methods.[12, 14, 15] In neutron matter, though, the finite range of the potential reduces Δ/E_F as the density increases. We find a ratio Δ/Δ_{BCS} that increases slightly from $|k_F a| = 1$ to 2.5, but thereafter remains roughly constant.

In Fig. 5 we compare the neutron matter results of Ref. [44] to selected previous results: a Correlated-Basis Function calculation by Chen *et al.* [33], an extension of the polarization-potential model by Wambach *et al.* [34], a medium-polarization calculation by Schulze *et al.* [35], a renormalization group calculation by Schwenk *et al.* [36], a Brueckner calculation by Cao *et al.* [39], a determinantal lattice QMC approach [42], and finally the newer Correlated-Basis Function calculation by Fabrocini *et al.* [38] that was used as an input wave function in the two AFDMC calculations of 2005 and 2008.[38, 41]

The results of our QMC calculations are much larger than most diagrammatic [33, 34, 35] and renormalization group [36] approaches. As these approaches assume a well-defined Fermi surface or calculate polarization corrections based on single-particle excitations it is not clear how well they can describe neutron matter in the strongly paired regime, or the similar pairing found in cold atoms. Ref. [39], which incorporates self-energy corrections
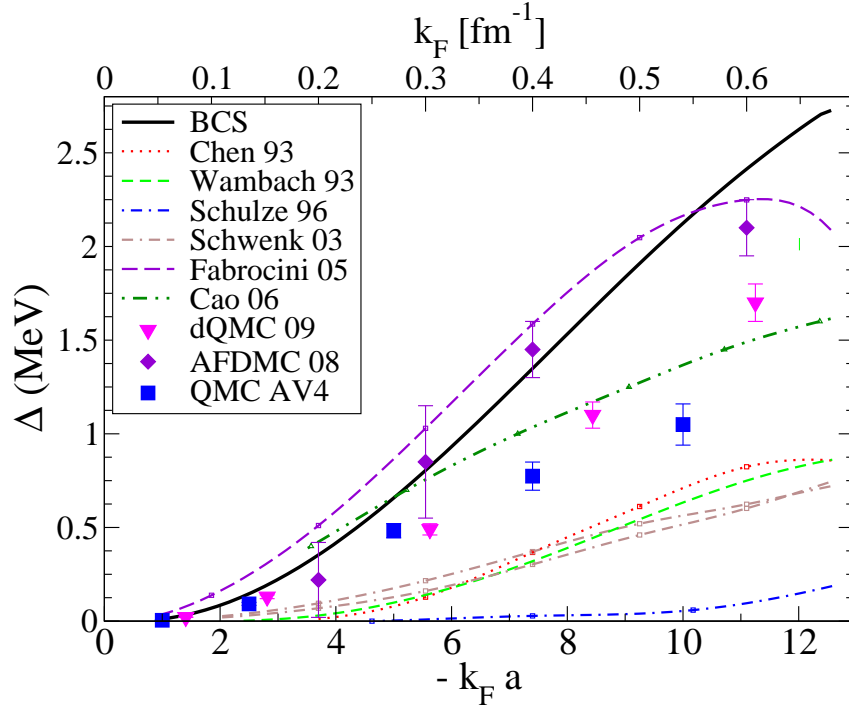
Figure 5. Superfluid pairing gap versus $k_F a$ for neutron matter compared to previous results.

and screening at the RPA level within Brueckner theory, appears to give results similar to ours. However, these values disagree with our lower-density results and, perhaps more importantly, at the lowest density reported the gap is larger than the mean-field BCS value (which is disallowed, as discussed in section 3.1.). On a similar note, Refs. [34] and [36] make use of a weak-coupling formula to calculate the pairing gap, similarly to Eqs. (3) and (4). The prefactor they use is justified based on predictions in the theory of ^{3}He. However, the concept itself of a Fermi surface is not well-defined in these strongly paired systems: in ^{3}He, in contrast to the present case, the gap is considerably smaller than the Fermi energy.

Having discussed the relationship of our QMC results to analytical approaches, a few comments on the relationship between the different extant simulation results are in order. The first AFDMC results for pairing gaps in neutron matter were published in Ref. [38]. These initial calculations were for very small system sizes of N=14-20 and yielded quite large pairing gaps. The AFDMC group then repeated their calculations for larger systems, [41] reducing the gap and eliminating part of the difference with GFMC results, but not entirely. Detailed explanations are given in Ref. [44]. The AFDMC approach includes a realistic two plus three nucleon interaction, and is therefore valuable for moderate to large densities. At very small densities we expect the s- and p-wave interactions to be sufficient. The trial wave function (and the constrained path approximation) for the AFDMC method are chosen from another approach. In the calculations of Refs. [38, 41] the wave function was taken from a Correlated-Basis Function (CBF) approach. This wave function is unre-

alistic at very low density as it yields a pairing gap larger than the Fermi energy. The QMC AV4 results use a wave function that has been variationally optimized, but a much simpler Hamiltonian that should nevertheless be valid at the lowest densities. Ref. [44] demonstrates that QMC calculations of the gap can be quite sensitive to the trial function, for example using the CBF input wave function the QMC calculation reproduces the AFDMC result for the pairing gap. We expect the QMC results are more accurate at low densities, but at higher densities the full interaction treated with AFDMC is required, along with a careful study of the impact of the trial wave function.

Finally, the QMC results seem to qualitatively agree (at least for the lowest densities considered) with a determinantal Quantum Monte Carlo lattice calculation [42] which, however, only includes the s-wave component in the interaction (which is why they agree much better with the results of Ref. [15] than those of Ref. [44]). This implies that a consensus is emerging, in that both the GFMC and the dQMC approaches find a gap that is suppressed with respect to the mean-field BCS result but is still a substantial fraction of the Fermi energy.

6.   Conclusions and Future Directions

To conclude, we have calculated the equation of state and pairing gap of cold atoms and low-density neutron matter with the AV4 interaction from $|k_F a|$ from 1 to 10. The calculated equation of state and pairing gap match smoothly with the known analytic results at low densities, and provide important constraints in the strong-coupling regime at large $k_F a$. The low-density equation of state can help constrain Skyrme mean-field models of finite nuclei. The pairing gap for low-density neutron matter is relevant to Skyrme-Hartree-Fock-Bogoliubov calculations [29] of neutron-rich nuclei and to neutron-star physics, since it is expected to influence the behavior of the crust. [26] Moreover, a magnetic field in the neutron star crust would have to be approximately 10^{17} G to overcome this gap and thus polarize neutron matter; such a value of the magnetic field is not implausible within the context of magnetars. The question of polarized neutron matter also has a long history [60] and has recently been attacked using Quantum Monte Carlo. [61, 62] Similarly, the fact that the magnitude of the gap is not as small as previously expected implies that a new mechanism that makes use of superfluid phonons is competitive to the heat conduction by electrons in magnetized neutron stars.[27]

This line of Quantum Monte Carlo calculations, having first been applied to and verified in cold atomic experiments, can also provide directions for future work in the field of nucleonic infinite matter. The simplest case is that of a two-component gas where the two populations are equal.[15, 44] The next step is to examine the ramifications of taking different populations for the two components: this is the case of spin-polarized low-density neutrons studied in Refs. [61, 62]. Cold-atom experiments have by now also addressed Efimov physics, in which three components are involved. In the nuclear context, adding a third species could provide further insight into the physics of neutron stars. If the third component particles were taken to be protons and, as in this paper, only a few of them were added, then it would be possible to study highly asymmetric nuclear matter. Another possible avenue of future research is related to optical lattice experiments with cold atoms: to first approximation these are equivalent to periodic external potentials. In the nuclear

case, an external potential would allow us to study the static response of neutron matter and would also facilitate the understanding of the impact on neutron pairing of the ion lattice that exists in a neutron star crust. Such microscopic results for the static response could provide further constraints on energy-density functionals used to describe the crust of neutron stars.

References

[1] J. Bardeen, Physics Today, p. 25 (December 1990).

[2] S. L. Shapiro and S. L. Teukolsky, *Black Holes, White Dwarfs, and Neutron Stars* (John Wiley & Sons Inc., New York, 1983).

[3] W. Ketterle and M. W. Zwierlein, in *Ultracold Fermi Gases*, Proceedings of the International School of Physics "Enrico Fermi," Course CLXIV, edited by M. Inguscio, W. Ketterle, and C. Salomon (IOS Press, Amsterdam, 2008). [arXiv:0801.2500]

[4] S. Giorgini, L. P. Pitaevskii, and S. Stringari, Rev. Mod. Phys. **80**, 1215 (2008).

[5] F. N. Magill, *The Nobel Prize winners. Physics* (Salem Press, Pasadena, 1989).

[6] A. B. Migdal, Nucl. Phys. **13**, 655 (1959).

[7] R. Grimm, in *Ultracold Fermi Gases*, Proceedings of the International School of Physics "Enrico Fermi," Course CLXIV, edited by M. Inguscio, W. Ketterle, and C. Salomon (IOS Press, Amsterdam, 2008). [arXiv:cond-mat/0703091]

[8] L. Luo and J. E. Thomas, J. Low Temp. Phys. **154**, 1 (2009).

[9] B. Marcelis, B. Verhaar, and S. Kokkelmans, Phys. Rev. Lett. **100**, 153201 (2008).

[10] G. F. Bertsch, *Many-Body Challenge Problem*, see R. F. Bishop, Int. J. Mod. Phys. B **15**, 10, iii, (2001).

[11] N. Navon, S. Nascimbène, F. Chevy, and C. Salomon, Science **328**, 729 (2010).

[12] J. Carlson *et al.*, Phys. Rev. Lett. **91**, 050401 (2003).

[13] G. E. Astrakharchik *et al.*, Phys. Rev. Lett. **93**, 200404 (2004).

[14] J. Carlson and S. Reddy, Phys. Rev. Lett. **95**, 060401 (2005).

[15] A. Gezerlis and J. Carlson, Phys. Rev. C **77**, 032801(R) (2008).

[16] M. M. Forbes, S. Gandolfi, and A. Gezerlis, Phys. Rev. Lett. **106**, 235303 (2011).

[17] M. W. Zwierlein (2011) talk presented at the Fermions from Cold Atoms to Neutron Stars Experimental Symposium, INT, Seattle, WA, May 16-20 2011.

[18] J. Carlson, S. Gandolfi, K. E. Schmidt, and S. Zhang, arXiv:1107.548 (2011).

[19] Y. Shin *et al.*, Nature **451**, 689 (2008).

[20] J. Carlson and S. Reddy, Phys. Rev. Lett. **100**, 150403 (2008).

[21] A. Schirotzek *et al.*, Phys. Rev. Lett. **101**, 140403 (2008).

[22] U. Lombardo and H.-J. Schulze, *Lecture Notes in Physics* (Springer-Verlag, Berlin, 2001), Vol. 578, p. 30.

[23] D. J. Dean and M. Hjorth-Jensen, Rev. Mod. Phys. **75**, 607 (2003).

[24] G. Baym, C. J. Pethick, and D. Pines, Nature **224**, 673 (1969).

[25] E. F. Brown and A. Cumming, Astrophys. J. **698**, 1020 (2009).

[26] D. Page, J. M. Lattimer, M. Prakash, and A. W. Steiner, Astrophys. J. **707**, 1131 (2009).

[27] D. N. Aguilera, V. Cirigliano, J. A. Pons, S. Reddy, and R. Sharma, Phys. Rev. Lett. **102**, 091101 (2009).

[28] B. A. Brown, Phys. Rev. Lett. **85**, 5296 (2000).

[29] N. Chamel, S. Goriely, and J.M. Pearson, Nucl. Phys. **A812**, 72 (2008).

[30] T. D. Lee and C. N. Yang, Phys. Rev. **105**, 1119 (1957).

[31] L. P. Gorkov and T. K. Melik-Barkhudarov, JETP, **40**, 1452 (1961) [Soviet Phys. JETP **13**, 1018 (1961)].

[32] H. -J. Schulze, A. Polls, and A. Ramos, Phys. Rev. C **63**, 044310 (2001).

[33] J. M. C. Chen, J. W. Clark, R. D. Davé, and V. V. Khodel, Nucl. Phys. **A555**, 59 (1993).

[34] J. Wambach, T. L. Ainsworth, and D. Pines, Nucl. Phys. **A555**, 128 (1993).

[35] H.-J. Schulze, J. Cugnon, A. Lejeune, M. Baldo, and U. Lombardo, Phys. Lett. **B375**, 1 (1996).

[36] A. Schwenk, B. Friman, and G. E. Brown, Nucl. Phys. **A713**, 191 (2003).

[37] H. Müther and W. H. Dickhoff, Phys. Rev. C **72**, 054313 (2005).

[38] A. Fabrocini, S. Fantoni, A. Y. Illarionov, and K. E. Schmidt, Phys. Rev. Lett. **95**, 192501 (2005).

[39] L. G. Cao, U. Lombardo, and P. Schuck, Phys. Rev. C **74**, 064301 (2006).

[40] J. Margueron, H. Sagawa, and K. Hagino, Phys. Rev. C **77**, 054309 (2008).

[41] S. Gandolfi, A. Yu. Illarionov, S. Fantoni, F. Pederiva, and K. E. Schmidt, Phys. Rev. Lett. **101**, 132501 (2008).

[42] T. Abe and R. Seki, Phys. Rev. C **79**, 054002 (2009).

[43] S. Gandolfi, A. Yu. Illarionov, F. Pederiva, K. E. Schmidt, and S. Fantoni, Phys. Rev. C **80**, 045802 (2009).

[44] A. Gezerlis and J. Carlson, Phys. Rev. C **81**, 025803 (2010).

[45] R. B. Wiringa, V. G. J. Stoks, and R. Schiavilla, Phys. Rev. C **51**, 38 (1995).

[46] V. A. Khodel, V. V. Khodel, and J. W. Clark, Nucl. Phys. **A598**, 390 (1996).

[47] A. Gezerlis, Ph.D. thesis, University of Illinois at Urbana-Champaign, 2009.

[48] R. B. Wiringa and S. C. Pieper, Phys. Rev. Lett. **89**, 182501 (2002).

[49] V. R. Pandharipande and H. A. Bethe, Phys. Rev. C **7**, 1312 (1973).

[50] B. Friedman and V. R. Pandharipande, Nucl. Phys. **A361**, 502 (1981).

[51] A. Akmal, V. R. Pandharipande, and D. G. Ravenhall, Phys. Rev. C **58**, 1804 (1998).

[52] J. Carlson, J. Morales, Jr., V. R. Pandharipande, and D. G. Ravenhall, Phys. Rev. C **68**, 025802 (2003).

[53] A. Schwenk and C. J. Pethick, Phys. Rev. Lett. **95**, 160401 (2005).

[54] J. Margueron, E. van Dalen and C. Fuchs, Phys. Rev. C **76**, 034309 (2007).

[55] M. Baldo and C. Maieron, Phys. Rev. C **77**, 015801 (2008).

[56] E. Epelbaum, H. Krebs, D. Lee, and U. -G. Meissner, Eur. Phys. J. A **40**, 199 (2009).

[57] E. Epelbaum, H.-W. Hammer, and U. -G. Meissner, Rev. Mod. Phys. **81**, 1773 (2009).

[58] A. Rios, A. Polls, and I. Vidaña, Phys. Rev. C **79**, 025802 (2009).

[59] K. Hebeler and A. Schwenk, Phys. Rev. C **82**, 014314 (2010).

[60] P. Haensel, Phys. Rev. C **11**, 1822 (1975).

[61] A. Gezerlis, Phys. Rev. C **83**, 065801 (2011).

[62] A. Gezerlis and R. Sharma, to be submitted (2011).